

# Control of Three-Dimensional Refractive Indices by Both Drawing and Poling of Functionalized Phenoxy Side-Chain Polymers

J. C. Kim,<sup>†</sup> T. Yamada,<sup>†</sup> C. Ruslim,<sup>†</sup> K. Iwata,<sup>‡</sup> T. Watanabe,<sup>†</sup> and S. Miyata<sup>\*,†</sup>

Graduate School of Bio-applications & Systems Engineering,  
Tokyo University of Agriculture and Technology, 2-24-16, Naka-machi, Koganei-shi,  
Tokyo 184, Japan, and Polymers & Materials Research Laboratories, Teijin Limited,  
4-3-2, Asahigaoka, Hino, Tokyo 191, Japan

Received February 21, 1996; Revised Manuscript Received June 27, 1996<sup>®</sup>

**ABSTRACT:** The novel functionalized side-chain polymer wherein *p*-nitrophenylcarbamate is imbedded into phenoxy resin backbone was synthesized. The orientation of the nonlinear optical chromophore of drawn and poled polymers was analyzed by measuring linear and nonlinear optical properties. The chromophore ratio, i.e., the ratio of monomer unit substituted by 4-nitrophenylcarbamate, was varied from about 28% to 100%, and then physical properties of polymers were characterized. The glass transition temperature ( $T_g$ ) increased up to 130 °C with increasing chromophore ratio due to the formation of hydrogen bonding. We demonstrated that the poling and drawing can control both the in-plane and out-of-plane birefringence by using the functionalized side-chain polymer having a large dipole moment  $\mu$  and linear molecular polarizability  $\alpha$ . The measurement of nonlinear optical properties was carried out to confirm the poling condition and orientation of polymer. The ideally uniaxially oriented films were poled parallel to the film-thickness direction by the contact poling method at  $T_g - 17$  °C. As the result, the out-of-plane birefringence ( $\Delta n_{Z-Y}$ ,  $X$  = drawing direction,  $Z$  = film thickness direction) of the drawn and poled polymer films was increased with increasing applied electric voltage and was independent of the draw ratio. It has been shown that most of the drawn and poled polymer films satisfy the relation of refractive indices such as  $n_X > n_Z > n_Y$ .

## Introduction

An anisotropic property of the oriented polymer can be described by the birefringence. Birefringence is, in particular, one of useful methods to measure the orientation state of an oriented amorphous polymer.<sup>1</sup> Accordingly, there had been many studies of molar refraction of polymers in 1950s.<sup>2</sup> However, computer simulation such as MOPAC (molecular package) has been recently used to calculate the birefringence of the polymer.<sup>3</sup> The refractive index of the polymer is related to the linear polarizability  $\alpha$ . Thus, for controlling the refractive index of the polymer, molecular polarizability should be considered in the molecular design level. For example, if a polymer representing positive birefringence has a large linear molecular polarizability in the main-chain direction and then it can be aligned, the refractive index of this oriented direction will be increased. With respect to this, drawing is one of the useful methods even though the molecular chains of the polymer are not aligned with the drawing direction exactly. If the molecular chains of the polymer are exactly aligned with the drawing direction, its mechanical properties may be greatly improved. By the way, drawing can only control the in-plane birefringence in the polymer; the refractive index  $n_X$  of the drawing direction can be controlled in the case of uniaxial drawing, and two refractive indices  $n_X$  and  $n_Y$  in two directions parallel to the plane and crossing each other at right angles can be controlled in the case of biaxial drawing. For example, a fiber can be only oriented uniaxially by drawing because refractive indices  $n_Y$  and

$n_Z$  cannot distinguish between themselves. The fiber is thus sufficient to consider two-dimensional refractive indices and then refractive index  $n_Z$  is not important. However, in the case of a polymer film, three-dimensional refractive indices should be considered. In-plane birefringence can only be controlled by drawing, but drawing is not sufficient to control the refractive index of the film-thickness direction  $n_Z$ . For example, uniaxially oriented Bisphenol A-polycarbonate (Bis-A PC) polymer film generally shows the relation of refractive indices such as  $n_X > n_Y = n_Z$ . Even if this film is drawn biaxially, refractive index  $n_Z$  of the film-thickness direction is much smaller than  $n_Y$ . Therefore a special method should be used to control the refractive index  $n_Z$  and to satisfy the relation of refractive indices such as  $n_X > n_Z > n_Y$ .

Several approaches to obtain the three-dimensional characteristics of the refractive index such as  $n_X > n_Z > n_Y$  have been reported in patents and scientific journals. There are also other special methods to control the refractive indices  $n_X$ ,  $n_Y$ , and  $n_Z$  in addition to drawing. The desired film is obtained by slicing an extruded rod and stretching it in the thickness direction in which the molecule is oriented.<sup>4</sup> The other method is a laminating method using a shrinkable film.<sup>5</sup> This method comprises laminating a resin film, i.e., the desired film, on one or both sides by a shrinkable polymer film such as poly(vinyl chloride) (PVC) or poly(ethylene terephthalate) (PET). Then this laminate is stretched while heating, so that the ability to shrink in the direction crossing the stretching direction is imparted to the resin film. Another method is film preparation under an electric or magnetic field.<sup>6</sup> After the polymer is oriented in the film-thickness direction in the film-preparation step, the polymer film is drawn.

<sup>†</sup> Tokyo University of Agriculture and Technology.

<sup>‡</sup> Teijin Ltd.

<sup>®</sup> Abstract published in *Advance ACS Abstracts*, September 1, 1996.

There is also a stacking method in which a stretched PC film representing positive birefringence is stacked with a stretched polystyrene (PSt) film representing negative birefringence.<sup>7</sup> However, all of these methods are incomplete because thickness control is difficult, the desired film size is limited, and the gained out-of-plane birefringence ( $\Delta n_{z-y}$ ) is very small, about 0.004. Therefore we have applied the poling technique, well used in nonlinear optics, as the alignment method to the polymer film having a large dipole moment in the side chain.

Poling is carried out to introduce noncentrosymmetric structure into the polymer in nonlinear optics (NLO) because second-order optical nonlinearity is not observed in isotropic media having a center of symmetry.<sup>8,9</sup> Even though polymers have a chromophore presenting large hyperpolarizability, they are not SHG active if a center of symmetry exists. In other words, when an external electric field is applied to the polymer film having an NLO chromophore with a dipole moment around the glass transition temperature, the dipole moments are aligned parallel to the direction of the electric field. It is found that macroscopic polarizability parallel to the applied external electric field is increased while a decrease occurs in the other directions. This phenomena is more effective when the polymer has a larger dipole moment. Polymers such as Bis-A PC and PSt fail to be completely aligned by poling because of their small dipole moments. But if an NO<sub>2</sub> group is bonded in the main chain or side chain, the total dipole moment becomes larger and their orientation by poling will be effective.

Accordingly, it may be possible to control three-dimensional anisotropy such as  $n_x > n_z > n_y$  by drawing and poling of a functionalized side-chain polymer, wherein a large molecular polarizability is introduced into the main chain to increase the in-plane birefringence and a large molecular polarizability and dipole moment are also introduced into the side chain to increase the out-of-plane birefringence. In this paper, we synthesize the novel phenoxy polymers containing *p*-nitrophenylcarbamate as a side chain. The chromophore ratio, side chain having a large molecular polarizability  $\alpha$ , and dipole moment  $\mu$  are varied to confirm the effect of the chromophore ratio on birefringence. After the characterization of materials, the nonlinear optical measurements are carried out to find the optimum poling conditions and superstructure of the polymer chain. Furthermore, three-dimensional anisotropic variation by drawing and poling is discussed.

## Experimental Section

**Polymer Synthesis.** The novel polymers were synthesized as shown in Figure 1. Phenoxy resin having an average molecular weight ( $M_w$ ) of 75 000 was obtained from Tohto Kasei Co. Ltd., and the other reagents were obtained commercially. Phenoxy resin was dissolved in THF and purified by precipitation in methanol. Tetrahydrofuran (THF) as solvent was distilled twice under the reduced pressure before use<sup>10</sup> and di-*n*-butyltin dilaurate was used as the catalyst. A three-necked flask was charged with 44.4 g (0.156 mol: relatively 1 mol against 4-nitrophenyl isocyanate) of phenoxy resin, 15.38 g (0.094 mol: relatively 0.6 mol against phenoxy resin) of *p*-nitrophenyl isocyanate, and 400 mL of THF; the slightly yellowish solution thus obtained was stirred at 70 °C for 9 h. The polymer was purified by precipitation in methanol three times after dissolving in THF and dried in a vacuum oven at 100 °C for 2 days after extraction in a rotary evaporator to remove methanol. In the same procedure, the mole ratio of *p*-nitrophenyl isocyanate against 1 mol of phenoxy resin

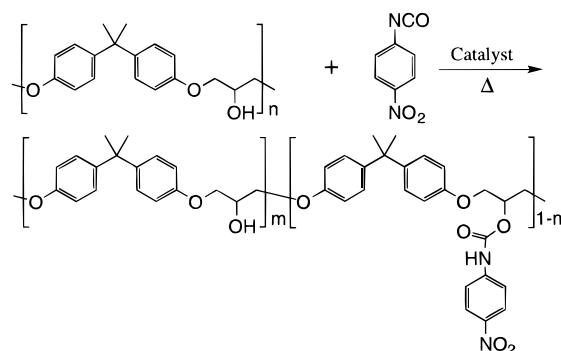


**Figure 1.** Synthetic scheme of functionalized side-chain polymers.

varied from 0.4 to 1.1 mol. All of these polymers were slightly yellow powder and could easily dissolve in THF, 1,4-dioxane, and dimethylformamide (DMF).

**Nonlinear Optical Measurements.** In order to investigate the optimum poling condition, thin films with 1  $\mu$ m thickness were prepared by spin coating on a soda lime glass from 10 wt % 1,4-dioxane solution. These spin-coated films were dried in a vacuum oven for 3 days with increasing temperature. The thickness and refractive indices of the films were determined by DEKTAK IIA and the prism-coupling method.<sup>11-13</sup>

A high positive voltage in the range of 4–9 kV was applied to the spin-coated films by the corona poling technique wherein the evaporated aluminum layer about 0.05  $\mu$ m on the other side was used as the ground electrode. After poling, the evaporated aluminum electrode was removed by a potassium hydroxide (KOH) solution for other measurements. Poling temperature was optimized during in-situ second harmonic generation (SHG) measurement. The chromophore orientation of the polymers was analyzed by a UV/visible spectrophotometer before and after poling. The setup for in-situ SHG measurement was similar to that described earlier by us,<sup>14,15</sup> and the irradiating Q-switched Nd:YAG laser beam (1064 nm, 10 ns/pulse, 10 Hz) was used. Nonlinear optical coefficients of polymer films were measured by the Maker fringe method. The Maker fringe data were analyzed by fitting parameters to the appropriate theoretical formula.<sup>16,17</sup>

**Drawing and Poling.** The films with about 70  $\mu$ m thickness were prepared by the cast method on a glass plate from 25 wt % 1,4-dioxane solution. These solvent-cast films were dried in a vacuum oven for 10 days with increasing temperature. To obtain isotropic polymer films, these cast films were dried above the  $T_g$  temperature under about  $10^{-1}$  Torr. After first drying, cast films on the substrate were put into a water bath of 60 °C for 5 h. The cast films were peeled off, and then these films, were fixed on the small glass frame by tape. These films were dried in the vacuum oven under the same temperature step of the first drying condition. These isotropic films were uniaxially drawn near the  $T_g$  temperature by a tensile tester. The draw rate is set to 2 mm/min to obtain the ideally uniaxially oriented films ( $n_x > n_y = n_z$ ). The draw ratio, here defined as the ratio of the final length of the drawn film in the stretching direction relative to the length before stretching, was varied from 1.3 to 2.3. The thickness and refractive indices of the pristine and drawn films were determined by a dial gauge and KS Optical Birefringence analyzer (KOBRA-21ADH, New Oji Paper Co. Ltd.).

The thicker pristine and drawn polymer films were poled by the contact poling method. The evaporated aluminum layers on both sides of the film were used as electrodes. A positive electric field of 75–150 V/ $\mu$ m was applied to the these films at room temperature, and the temperature was heated to about  $T_g$  - 17 °C and maintained for 2 h. The film is then cooled to room temperature in the presence of the electric field, and this electric field was finally removed. After poling, the evaporated aluminum electrodes were removed by KOH solution to measure other measurements. The refractive indices were measured by the same instrument.

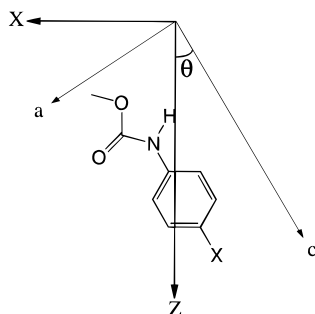


**Figure 2.** Chemical formula of methyl *N-p*-R-substituted phenylcarbamate and coordinate axes in the aromatic plane. The *ac* plane also lies in the *XZ* plane.

## Results and Discussion

**Molecular Design.** In molecular design of a functionalized side-chain polymer, the choice of side chain, i.e., chromophore, is important. The molecular polarizability  $\alpha$  and dipole moment  $\mu$  of the chromophore should be considered. Furthermore, it is necessary to select the chromophore having a large polarizability and dipole moment in the same direction. According to this molecular design concept, we selected some chromophores of a quasiplanar structure<sup>18</sup> such as *p*-nitroaniline and the selected chromophores are methyl *N*-phenylcarbamate ( $R = H$ ), methyl *N-p*-nitrophenylcarbamate ( $R = NO_2$ ), methyl *N-p*-bromophenylcarbamate ( $R = Br$ ), and methyl *N-p*-fluorophenylcarbamate ( $R = F$ ). Using these chromophores, the theoretical polarizability according to the applied external electric field was calculated using MOPAC. However MOPAC calculation results are presented on the Cartesian coordinate, so they differ from the effective polarizability according to the applied external electric field. Thus the coordinate system is translated to achieve the effective polarizability. The relation of the coordinate system is represented by Figure 2. The effective polarizability  $P_Z$  of the *Z* direction according to the applied external electric field ( $E_Z$ ) can be represented as follows:

$$P_Z = \alpha_{ZZ} E_Z \quad (1)$$

Furthermore  $P_Z$  based upon Figure 2 can be expressed as follows:

$$P_Z = \cos \theta P_c + \sin \theta P_a \quad (2)$$

where  $P_a$  and  $P_c$  are the calculated polarizability from MOPAC. Polarization occurs according to the applied external electric field  $E_a$  and  $E_c$  and can be given as follows:

$$\begin{pmatrix} P_a \\ P_b \\ P_c \end{pmatrix} = \begin{pmatrix} \alpha_{aa} & \alpha_{ab} & \alpha_{ac} \\ \alpha_{ba} & \alpha_{bb} & \alpha_{bc} \\ \alpha_{ca} & \alpha_{cb} & \alpha_{cc} \end{pmatrix} \begin{pmatrix} E_a \\ E_b \\ E_c \end{pmatrix} \quad (3)$$

Since the off-diagonal components on the matrix are approximately  $1/100$ th when compared to diagonal components, they may be ignored. Therefore, polarizabilities  $P_a$  and  $P_c$  are

$$\begin{aligned} P_a &= \alpha_{aa} E_a, & P_c &= \alpha_{cc} E_c \\ \therefore P_Z &= \alpha_{cc} \cos \theta E_c + \alpha_{aa} \sin \theta E_a \end{aligned} \quad (4)$$

The applied external electric fields  $E_a$  and  $E_c$  can be illustrated on the basis of  $\theta$  and the applied external

**Table 1. Theoretical Results of Methyl *N-p*-R-Substituted Phenylcarbamate**

R	H	NO <sub>2</sub>	F	Br
$\mu$ (Debye)	2.12	7.00	3.08	2.76
$\alpha_{cc}$ ( $\times 10^{-23}$ esu)	3.95	5.06	4.12	5.13
calc $\alpha_{ZZ}$ ( $\times 10^{-23}$ esu)	2.74	4.76	3.28	3.60
$\lambda_{cutoff}$ (nm) <sup>a</sup>	290	350	290	300

<sup>a</sup> It was calculated by ZINDO.

electric field  $E_Z$ , so eq 4 is

$$P_Z = (\alpha_{cc} \cos^2 \theta + \alpha_{aa} \sin^2 \theta) E_Z \quad (5)$$

When the eq 1 is compared with eq 5, effective polarizability  $\alpha_{ZZ}$  occurring according to the applied external electric field  $E_Z$  is

$$\alpha_{ZZ} = \alpha_{cc} \cos^2 \theta + \alpha_{aa} \sin^2 \theta \quad (6)$$

Angle  $\theta$  can be calculated on the basis of the scalar sum of the strength of dipole moment of the *a* and *c* directions of chromophore. Furthermore, for polarizabilities  $\alpha_{cc}$  and  $\alpha_{aa}$ , the results calculated with the molecular orbital calculation MOPAC PM3<sup>19</sup> were used. The results of the calculation for the chromophores selected as mentioned above are shown in Table 1. The cutoff wavelength of those chromophores could be calculated with the molecular orbital calculation ZINDO (Professor M. C. Zerner's INDO (Intermediate Neglect of Differential Overlap<sup>20</sup>) program). ZINDO was developed at the University of Florida Quantum Theory Project. ZINDO provides two different valence-electron-only semiempirical procedures: a method for computing spectroscopic properties (electronic spectra) and a method of computing molecular geometries (conformations and structures). Especially, in a method for computing spectroscopic properties (electronic spectra) the UV/visible spectrum can be computed. Of the four chromophores, the effective polarizability of methyl *N-p*-nitrophenylcarbamate was the largest, and its value was about  $4.76 \times 10^{-23}$  esu. The  $\alpha_{cc}$  of methyl *N-p*-nitrophenylcarbamate was nearly identical with that of methyl *N-p*-bromophenylcarbamate; however it can be oriented by the external electric field parallel to the direction of the external electric field larger than methyl *N-p*-bromophenylcarbamate because methyl *N-p*-nitrophenylcarbamate has a much larger dipole moment than *N-p*-bromophenylcarbamate. Thus methyl *N-p*-bromophenylcarbamate may not be effective in the poling although having large molecular polarizability  $\alpha_{cc}$ . Incidentally, the polymer synthesized by phenoxy polymer and methyl *N-p*-nitrophenylcarbamate might appear slightly pale yellow because the cutoff wavelength of this chromophore was presented in the near-visible range. However, we selected this polymer for the characterization of the drawing and poling effect because it may show a large polarizability by poling parallel to the poling direction.

**Characterization of Polymers.** The chemical structure of polymers was characterized by <sup>1</sup>H-NMR and FT-IR. The ratio of 4-nitrophenylcarbamate substituted in phenoxy resin, namely chromophore ratio, was varied from about 28% to 100%. The proton peak of carbon linked with an -OH group in the main chain was changed from 5.2 to 5.4 ppm according to the substituting chromophore, as shown in Figure 3. In the FT-IR spectra, the absorption peak of the carbonyl group at

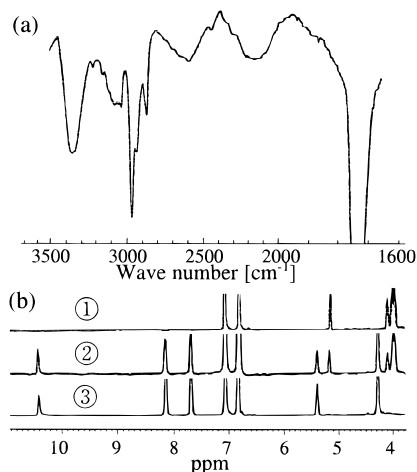


**Figure 3.** Characterization of the polymers: (a) FT-IR spectrum (0.99 chromophore ratio); (b) NMR spectra (DMSO- $d_6$ ) measured by 400 MHz NMR at 60 °C as a function of chromophore ratio ( $1 - m$ ) (1) 0, (2) 0.52, and (3) 0.99, respectively.

**Table 2. Basic Properties of Polymers**

chromophore ratio ( $1 - m$ )	$T_g$ (°C)	$\lambda_{\text{cutoff}}^a$ (nm)	density <sup>b</sup> (g/cm <sup>3</sup> )	refractive index <sup>c</sup>
0 <sup>d</sup>	95	305	1.2038	1.5985
0.33	114	420	1.2184	1.6090
0.52	122	425	1.2332	1.6144
0.72	127	430	1.2489	1.6169
0.99	130	450	1.2636	1.6219

<sup>a</sup> The cutoff wavelength defined as the onset wavelength of the absorption peak at the longer wavelength side. <sup>b</sup> The densities were measured by a pycnometer at room temperature. <sup>c</sup> Refractive indices were measured at the Na D-line (589.3 nm) at 20 °C. <sup>d</sup> 0 means phenoxy resin itself.

1740  $\text{cm}^{-1}$  increased with the increasing chromophore ratio. The absorption peak of the amine group appeared at 3350  $\text{cm}^{-1}$  and hydrogen bonding formation was characterized compared with free amine absorption peak at 3450  $\text{cm}^{-1}$ . The basic properties of polymers are shown in Table 2. The glass transition temperature ( $T_g$ ) of these polymers increased to 130 °C with the increasing chromophore ratio because of hydrogen bonding formation, while the  $T_g$  temperature of the polymer substituted by a side chain such as the benzoyl group was decreased with the increasing esterification ratio.<sup>21</sup> This phenomenon of  $T_g$  temperature increase due to hydrogen bonding formation also appeared in the phenoxy polymer containing the  $\alpha$ -cyano unsaturated carboxylate.<sup>22</sup> The  $T_g$  temperature of the phenoxy polymer containing the  $\alpha$ -cyano unsaturated carboxylate was increased to 123 °C. The cutoff wavelength of the synthesized polymer was largely shifted compared with that of the phenoxy polymer due to the introduction of the nitro group. As a result, the color of the synthesized polymer film having about 100% chromophore ratio was yellowish. Before decomposition, no melting peak was observed in these polymers, indicating that they are amorphous.

**Confirmation of Poling Effect.** To find the optimum poling temperature, in-situ SHG measurements were carried out as shown in Figure 4. In-situ SHG experiments measure SHG intensity as a function of the temperature. According to the increasing temperature, chromophores of the polymer chains are aligned parallel to the direction of the applied electric field, so that a noncentrosymmetric structure is being made by poling.

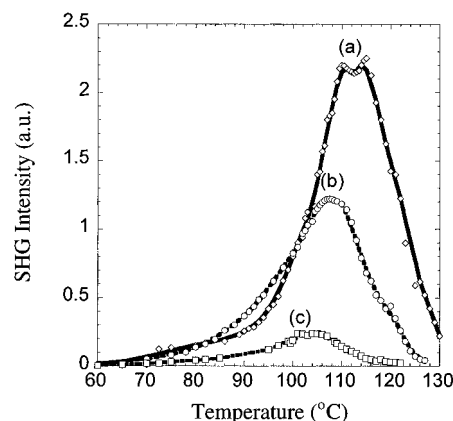


**Figure 4.** In-situ SHG measurements of the polymer films having chromophore ratio ( $1 - m$ ) (a) 0.99, (b) 0.72, and (c) 0.52, respectively.

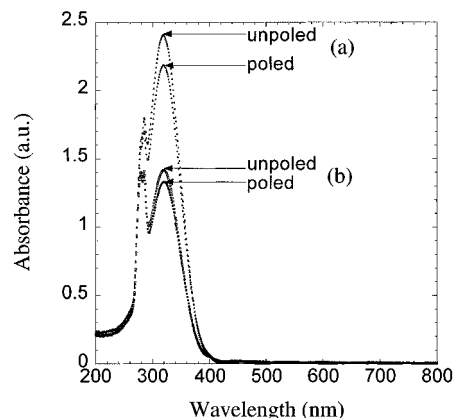


**Figure 5.** UV/visible absorption spectra of the polymers before and after poling and the corresponding chromophore ratio ( $1 - m$ ): (a) 0.99; (b) 0.52.

The SHG signal is proportional to a degree of poling effect, and the SHG signal would typically reach a plateau and then decrease as the ionic conductivity of the polymer film increased, reducing the internal electric field.<sup>23</sup> The optimum poling temperature was determined from a temperature at which the SHG plateau was observed. Thus the optimum poling temperature of the spin-coated films having different chromophore ratios was increased with the increasing chromophore ratio, but the temperatures were almost 17 deg lower than the glass transition temperature. Considering this, poling above  $T_g - 17$  °C may not be effective for chromophore orientation and thus the optimum poling temperature is determined to be  $T_g - 17$  °C.

The absorption spectra of polymer films before and after corona poling were measured with a UV/visible spectrophotometer in the wavelength range 200–800 nm, as shown in Figure 5. After poling, a decrease in absorbance (hypochromic shift) was observed in all polymers, and the decreasing ratio was increased with the increasing chromophore ratio. The decrease in absorbance after poling is due to the alignment of the chromophore. During corona poling, the surface charge is accumulated on the surface of the polymer films with opposite charge at the planar electrode,<sup>24</sup> and this introduces a large electrostatic field in the film that interacts with the chromophores of the polymer. The static field aligns the dipoles in the direction of the poling field, which leads to a change in the intensity of the absorption spectrum, i.e., dichroism. One parameter

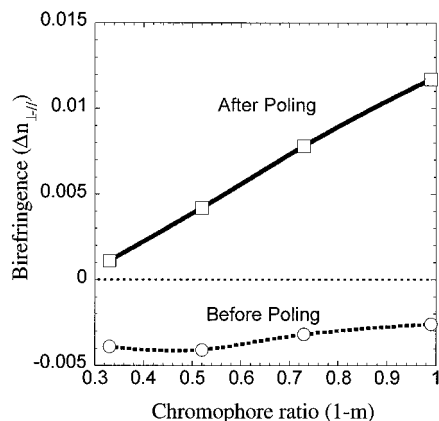


**Figure 6.** Birefringence of spin-coat films before and after corona poling measured by the prism-coupling method at 632.8 nm.

to express the extent of poling-induced orientation is the order parameter shown:

$$\Theta = 1 - A_p/A_0 \quad (7)$$

where  $A_p$  is the absorbance perpendicular to the poling direct of a poled film and  $A_0$  is the absorbance of an unpoled polymer film. The order parameter was determined to be 0.10 at about 0.99 chromophore ratio and 0.05 at about 0.54 chromophore ratio, and it also increased with the increasing chromophore ratio.

The refractive indices of polymers were measured by the prism-coupling method in a slab waveguide configuration, the results of which were plotted in Figure 6. In the waveguide technique the birefringence can be expressed as the difference between  $n_{||}$  and  $n_{\perp}$ .  $n_{||}$  is the refractive index of the sample in the direction along the film plane, and  $n_{\perp}$  is the refractive index in the direction perpendicular to the film plane. The value of birefringence was determined by the orientation of the chromophores and steric constraints in the films. In these polymer films, the refractive indices of  $n_{\perp}$  become larger than those of  $n_{||}$  by corona poling. Namely, birefringence ( $n_{\perp} - n_{||}$ ) induced by corona poling was found to be in the range 0.005–0.014, as shown in Figure 6. These results mean that, before poling, the polymer chains are preferentially stretched along the film plane. When a strong electric field such as corona discharge is applied to the films, the chromophores are aligned along the field direction.

**Superstructure Analysis Using Nonlinear Optical Properties.** Nonlinear optical properties of both drawn and poled polymer films were studied to analyze the superstructure. The isotropic polymer films having 0.99 chromophore ratio were poled by the contact poling method at 75 and 150 V/ $\mu$ m. And the same isotropic polymer films were uniaxially drawn about 1.8 times and poled at the same poling conditions. Using these films, nonlinear optical coefficients were measured by the Maker fringe method. Maker fringes for both the s- and p-polarized fundamental and the p-polarized second harmonic of pristine and poled polymer films were measured. The pristine and poled polymer belongs to the  $\infty mm$  point group, representing two independent nonlinear optical coefficients,  $d_{33}$  and  $d_{31}$ , because of Kleinman symmetry, and is changed to the  $mm2$  point group by drawing. For a system with a  $mm2$  point group the nonlinear polarization  $P_{NL}$ <sup>25,26</sup> is given by

$$P_{NL} = \begin{bmatrix} 0 & 0 & 0 & 0 & d_{15} & 0 \\ 0 & 0 & 0 & d_{24} & 0 & 0 \\ d_{31} & d_{32} & d_{33} & 0 & 0 & 0 \end{bmatrix} \begin{bmatrix} E_1^2 \\ E_2^2 \\ E_3^2 \\ 2E_2E_3 \\ 2E_1E_3 \\ 2E_1E_2 \end{bmatrix} \quad (8)$$

where there are five nonzero  $d$  coefficients. Under the Kleinman symmetry restriction, we have

$$d_{31} = d_{15}, \quad d_{32} = d_{24} \quad (9)$$

The second-order NLO properties are finally governed by the three independent nonzero coefficients. These coefficients can be determined by the Maker fringe method, and the Maker fringes obtained and the corresponding sample schemes are shown in Figure 7.<sup>27,28</sup> Thus Maker fringes for both the s- and p-polarized fundamental and the p-polarized second harmonic of drawn and poled polymer films are measured in the drawing direction and perpendicular direction against the drawing direction, an example of which is shown in Figure 7. Here  $\Phi$  is the angle between the propagation direction and the normal to the film surface. The SHG intensity is zero at  $0^\circ$  and grows symmetrically around this angle, indicating that after poling the average dipole moment of the polymer is perpendicular to the film surface. The nonlinear optical coefficients can be estimated by fitting the measured SHG intensities in both p-p and s-p polarization compared with the Y-cut quartz reference,<sup>29</sup> and the calculated results are shown in Table 3. Refractive indices at 1.064 and 0.532  $\mu$ m were measured by the prism method. The  $d_{33}$  value of the pristine and poled polymer film was increased from 2.4 to 4.0 pm/V with the increasing applied electric voltage. By drawing, this  $d_{33}$  value was increased from 3.6 to 6.8 pm/V with the increasing applied electric voltage. And  $d_{33}$  values of most films were about 3 times as large as  $d_{31}$ , such that  $d_{33} = 3d_{31}$ ;<sup>30</sup> however one film drawn and poled at 150 V/ $\mu$ m showed  $d_{33}$  about 5 times as large as  $d_{31}$ . These results mean that the main chains of the polymer may be better aligned by drawing and the orientation of chromophores by poling may be easy due to the decrease of steric hindrance. Kuzyk et al.<sup>31</sup> stated that tensor ratio  $a$  ( $a = d_{31}/d_{33}$ ) can be controlled with stress; a large  $d_{31}$  value was obtained whereas the  $d_{33}$  value was decreased in their experiment because the polymer film was poled and pressured in the same direction. We also confirmed similar phenomena presented by Kuzyk et al.<sup>31</sup> in which tensor ratio  $a$  can be controlled by drawing and poling. Tensor ratio  $a$  of the poled film under stress was found to be 0.70 by Kuzyk et al., whereas we found that it decreased to 0.29 when the films were poled in the influence of 150 V/ $\mu$ m and drawn perpendicular to the poling direction. This means that a larger  $d_{33}$  value relative to  $d_{31}$  was obtained and the chromophore of the polymer can be more easily oriented by poling and uniaxial drawing. Therefore, the tensor ratio  $d_{31}/d_{33}$  of drawn and poled films can be controlled. The ratios  $d_{31}/d_{32}$  of all poled polymer films were found to be 1 and not changed by drawing. These results suggest that the chromophore would be randomly oriented along the in-plane direction of the polymer. And both  $d_{31}$  and  $d_{32}$  values of polymer films poled in the influence of 150 V/ $\mu$ m were about 2 times larger than that at 75 V/ $\mu$ m. These results suggest that chromophores were oriented

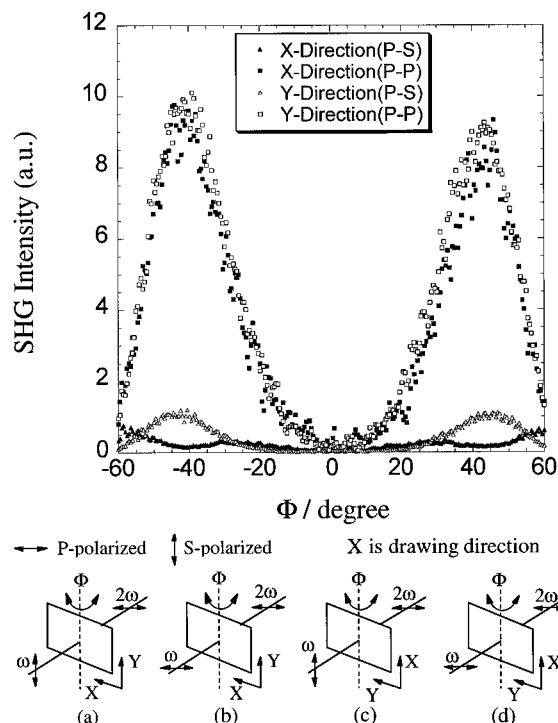


**Figure 7.** Maker fringes of drawn poled polymer film with P-P and P-S polarization at the drawing direction and its perpendicular direction. The chromophore ratio of the polymer film with 46  $\mu\text{m}$  was 0.99, the draw ratio was 1.8, and the applied electric field was 150 V/ $\mu\text{m}$ . The nonlinear coefficients corresponding to each configuration are (a)  $d_{32}$ , (b)  $d_{31}$  and  $d_{33}$ , (c)  $d_{31}$ , and (d)  $d_{32}$  and  $d_{33}$ .

**Table 3. Nonlinear Optical Coefficients<sup>a</sup> of the Solvent-Cast Polymer Films Having 0.99 Chromophore Ratio (1 -  $m$ )**

	drawn and poled film		pristine and poled film	
	75 V/ $\mu\text{m}$	150 V/ $\mu\text{m}$	75 V/ $\mu\text{m}$	150 V/ $\mu\text{m}$
$d_{33}$	$3.6 \pm 0.51$	$6.8 \pm 0.95$	$2.4 \pm 0.35$	$4.0 \pm 0.59$
$d_{31}$	$0.7 \pm 0.09$	$1.4 \pm 0.21$	$0.7 \pm 0.11$	$1.1 \pm 0.17$
$d_{32}$	$0.5 \pm 0.08$	$1.2 \pm 0.22$		

<sup>a</sup>  $d_{11}(\text{quartz}) = 0.4 \text{ pm/V}$ .

more to the direction of the applied electric field according to the increasing poling field.

**Change of Refractive Indices by Drawing and Poling.** The thicker films to confirm the control of the refractive index by drawing and poling were prepared by the solvent-cast method. All prepared films showed the isotropic relation of the refractive index such as  $n_X = n_Y = n_Z$  because the polymer chains were randomly oriented by drying above  $T_g$  for 2 days. Then these isotropic films were uniaxially drawn by tensile tester. Refractive indices of all films were evaluated from the measurement of film retardation  $R$ . It can be expressed as follows:

$$R = \Delta n d \quad (10)$$

where  $\Delta n$  is the birefringence and  $d$  is the thickness of the film. Therefore, if the thickness of the film is known, the birefringence can be gained. When the linear-polarized light is transmitted perpendicular to the plane of film surface, retardation  $R_0$  composed in-plane birefringence  $n_X - n_Y$  and in-plane birefringence can be calculated. When the incident linear-polarized light is illuminated with incident angle  $\theta$  by rotating the film around the  $Y$ -axis,  $n_Z$  is composed to the

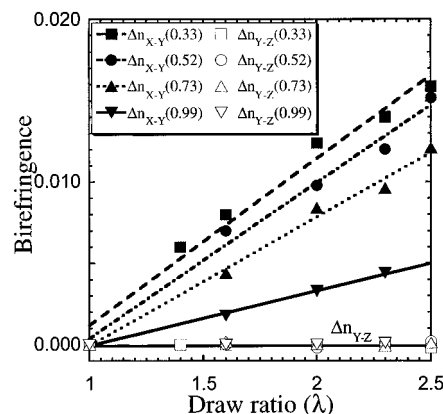


**Figure 8.** Change of birefringence by uniaxial drawing. The drawing temperature was about the  $T_g$  temperature, and the drawing rate was 2 mm/min. The values in the legend refer to the chromophore ratio (1 -  $m$ ).

retardation  $R_\theta$ , and  $R_\theta$  is expressed as follows:

$$R_\theta = (n_x - n_y) d / \cos \alpha \quad (11)$$

$$n_\alpha^2 = n_x^2 n_z^2 / (n_x^2 \sin^2 \alpha + n_z^2 \cos^2 \alpha) \quad (12)$$

where  $\alpha$  is the refractive angle. The refractive angle  $\alpha$  can be calculated by Snell's law as follows:

$$n_\alpha \sin \alpha = \sin \theta \quad (13)$$

where  $n$  is the average refractive index,  $n$  can be measured by an Abbé refractometer using the Na D-line (589.3 nm) at 20 °C and is expressed as follows:

$$n = (n_X + n_Y + n_Z) / 3 \quad (14)$$

Thus refractive indices  $n_X$ ,  $n_Y$ , and  $n_Z$  of the drawn and poled polymer films can be derived by solving eqs 10–14.

The uniaxially drawn films showed the relation of the refractive index such as  $n_X > n_Y = n_Z$ , as shown in Figure 8. These results mean that chromophores are cylindrically oriented around the main chain of the polymer. The slopes of the in-plane birefringence ( $\Delta n_{X-Y}$ ) were decreased with the increasing chromophore ratio because the macroscopic linear polarizabilities of chromophores in the  $Y$ - and  $Z$ -directions become larger according to the increase of the chromophore ratio, and then the in-plane birefringence become smaller.

The uniaxially oriented films were polarized by contact poling. The range of applied electric voltage that could be sustained without breakdown was varied from 75 to 150 V/ $\mu\text{m}$ , and the optimum poling temperature, i.e.,  $T_g - 17$  °C, was decided by in-situ SHG measurement. The out-of-plane birefringences ( $\Delta n_{Z-Y}$ ) of the drawn and poled polymer films as a function of applied electric field were shown in Figure 9. The out-of-plane birefringence generally tended to increase with the increasing chromophore ratio; especially, the out-of-plane birefringence of the film poled at the 150 V/ $\mu\text{m}$  applied electric field was only increased in proportion to the chromophore ratio. The slopes of the fitting line of the out-of-plane birefringence in the case of each electric field were varied with the increasing electric field and the change of slope in the case of 75 V/ $\mu\text{m}$  was smaller than that at 150 V/ $\mu\text{m}$ . These results indicate that the out-of-plane birefringence variation depends on the chromophore ratio. We thought that the reason

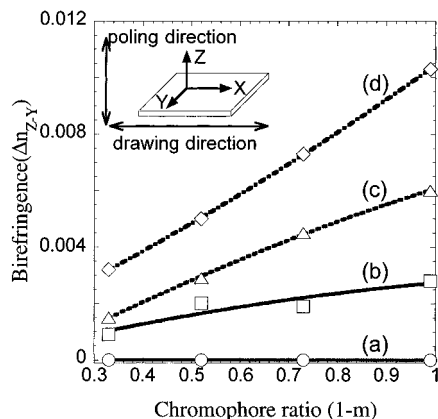


**Figure 9.** Out-of-plane birefringence ( $\Delta n_{Z-Y}$ ) as a function of the chromophore ratio and the applied electric field: (a) 0 V/ $\mu\text{m}$ ; (b) 75 V/ $\mu\text{m}$ ; (c) 100 V/ $\mu\text{m}$ ; (d) 150 V/ $\mu\text{m}$ . The poling temperature was  $T_g - 17^\circ\text{C}$ .

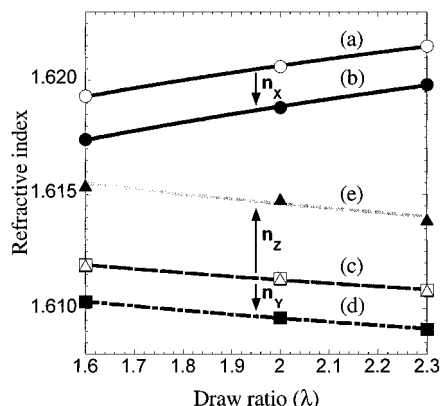


**Figure 10.** Refractive indices before and after poling: (a)  $n_x$  (before poling); (b)  $n_x$  (after poling); (c)  $n_y$  and  $n_z$  (before poling); (d)  $n_y$  (after poling); (e)  $n_z$  (after poling). The uniaxially drawn polymer films having 0.52 chromophore ratio were poled in the influence of 150 V/ $\mu\text{m}$  at  $T_g - 17^\circ\text{C}$ .

might be the increase of steric hindrance and hydrogen bonding formation of urethane bonds according to the increasing chromophore. The cylindrically aligned side chains of the uniaxially drawn polymer film can be aligned toward the direction of the applied electric field in the lower chromophore ratio by poling because the average distance between each chromophore is relatively long; then the effect of steric hindrance may be smaller, and hydrogen bonding formation between the polymer chains may be difficult. But while the chromophore ratio increases, the effect of steric hindrance is bigger and it may be possible to form hydrogen bonding between the polymer chains. We reported that the hydrogen bonding of polyurea was only broken under a high electric field but reconstructed hydrogen bonding after poling results in remanent polarization which exhibits ferroelectric properties and a stable SHG.<sup>32</sup> Thus, in our polymer system, chromophores can be aligned according to the cutting of the hydrogen bonding under a high electric field such as 150 V/ $\mu\text{m}$  and the hydrogen bonding is reconstructed after orientation.

The drawn polymer films as a function of the draw ratio were polarized by contact poling under the same conditions, and the change of refractive indices is shown in Figure 10. The refractive index  $n_z$  was increased whereas  $n_x$  and  $n_y$  were decreased according to the draw ratio because the side chains of the polymer can be aligned parallel to the applied electric field by poling.

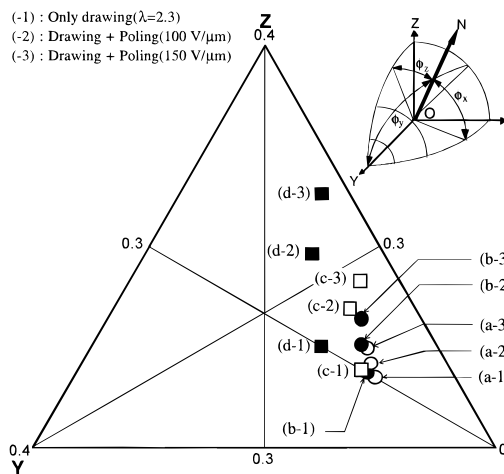


**Figure 11.** Equilateral triangle coordinates representing the degrees of the drawn and poled polymer films of the three quantities of  $\cos^2 \phi_i$ . Chromophore ratio (1 - m): (a) 0.33 (○); (b) 0.52 (●); (c) 0.72 (□); (d) 0.99 (■).

The increase of  $n_z$  by poling is a sum of the decrease of  $n_x$  and  $n_y$  because the refractive indices  $n_x$ ,  $n_y$ , and  $n_z$  are calculated using the average refractive index by the polarization analysis method. The interesting result was that the poling effect was independent of the draw ratio. Namely, the increase of  $n_z$  by poling was the same because the chromophores of each drawn polymer film were cylindrically oriented by ideally uniaxial drawing, as the relation of refractive indices showed  $n_x > n_y = n_z$ . The other drawn and poled polymer films showed the same results.

The molecular orientation of polymer films changed by drawing and poling can be, as in Figure 11, shown in the convenient equilateral triangular coordinate system described by Desper et al.<sup>33</sup> Three quantities  $\cos^2 \phi_i$  ( $i = X, Y, Z$ ), which are one of the representations for the molecular orientation, can be obtained by solving the following equation:<sup>34</sup>

$$n_i = (n_{\parallel} - n_{\perp}) \cos^2 \phi_i + n_{\perp} \quad (i = X, Y, Z) \quad (15)$$

where  $(n_{\parallel} - n_{\perp})$  is intrinsic birefringence  $\Delta^\circ$  (it is defined as the difference between the principal refractive index in the main-chain direction  $n_{\parallel}$  and the principal refractive index perpendicular to the main-chain direction  $n_{\perp}$ ) and  $n_i$  is the refractive indices measured in the three principal dielectric axes. Intrinsic birefringence  $\Delta^\circ$  can be calculated by the following approximated Lorentz-Lorenz relation:<sup>35</sup>

$$\Delta^\circ = \frac{2\pi}{9} \left( \frac{n^2 + 2}{n} \right)^2 N \Delta\alpha \quad (16)$$

where  $n$  is an average refractive index,  $N$  is the number of molecules per unit volume, and  $\Delta\alpha$  is the difference of the linear polarizability between that in the main-chain direction and that in the direction perpendicular to the main-chain direction. The values of  $\Delta\alpha$  were calculated by molecular orbital calculation. The sum of the three quantities is 1, and this means that only two of the three quantities are independent, the third being fixed. Perfect orientation of the molecular axis  $x$  parallel to the principal dielectric axis  $X$  maps onto the vertex of the equilateral triangle diagram, labeled  $X$  and

the three quantities are

$$\overline{\cos^2 \phi_X} = 1, \quad \overline{\cos^2 \phi_Y} = \overline{\cos^2 \phi_Z} = 0 \quad (17)$$

For orientation of the molecular axis  $x$  perpendicular to the principal dielectric axis  $X$  the three quantities are

$$\overline{\cos^2 \phi_X} = 0, \quad \overline{\cos^2 \phi_Y} + \overline{\cos^2 \phi_Z} = 1 \quad (18)$$

And random orientation of the polymer chains would map onto the center of the triangle where

$$\overline{\cos^2 \phi_X} = \overline{\cos^2 \phi_Y} = \overline{\cos^2 \phi_Z} = 1/3 \quad (19)$$

And uniaxial orientation of the molecular chains about the  $x$  direction maps onto the line bisecting the  $60^\circ$  angle at vertex  $X$ . In this case,

$$(1 - \overline{\cos^2 \phi_X})/2 = \overline{\cos^2 \phi_Y} = \overline{\cos^2 \phi_Z} \quad (20)$$

Three quantities  $\overline{\cos^2 \phi_i}$  ( $i = X, Y, Z$ ) were calculated and plotted as shown in Figure 11; however the equilateral triangular coordinate system having a scale from 0 to 1 was magnified up to 0.4 in order to emphasize the difference of each datum because these values were very small. These points of drawn and poled films mean either that drawn and poled films were oriented smaller than intrinsic birefringence or that calculated intrinsic birefringence was overestimated by the molecular orbital method. In Figure 11, the data (a-1), (b-1), (c-1), and (d-1), of all polymer films drawn about 2.3 times show that polymer films were uniaxially drawn, and the change of the data position according to the chromophore ratio coincides with the result of Figure 8. And in-plane birefringences of the drawn polymer films of 0.99 chromophore ratio, representing data (d-1), were smaller than those of the other drawn films since the chromophore having a polarizability larger than that of the main chain is cylindrically oriented around the main chain and then the drawing effect thereof would not become larger. The data of drawn and poled films map onto the position tilted to the vertex of the equilateral triangle diagram, labeled  $Z$ , and the position is more moved to the  $Z$  vertex by the higher poling field. For example, the out-of-plane birefringence of the drawn polymer film (d-1) was increased to (d-2) or (d-3) according to the applied poling field. Such results mean that the drawn and poled films were biaxially oriented in the film-thickness direction due to the orientation of the chromophore and that the orientation of the chromophore is larger corresponding to the strength of the applied external electric field.

Figure 12 shows the three-dimensional anisotropic variation of the polymer films by drawing and poling according to the chromophore ratio, and these drawn polymer films wherein the draw ratio was about 2.3 times poled under the same conditions. The increase ratio of the refractive indices, after these drawn polymer films were poled, was larger with the increasing chromophore ratio. Almost drawn and poled polymer films showed the relation of refractive indices such as  $n_X > n_Z > n_Y$ , but the drawn and poled polymer films having the 0.99 chromophore ratio showed the relation of the refractive indices such as  $n_Z > n_X > n_Y$ . Accordingly, we confirmed that in-plane and out-of-plane birefringence can be simultaneously controlled by both drawing

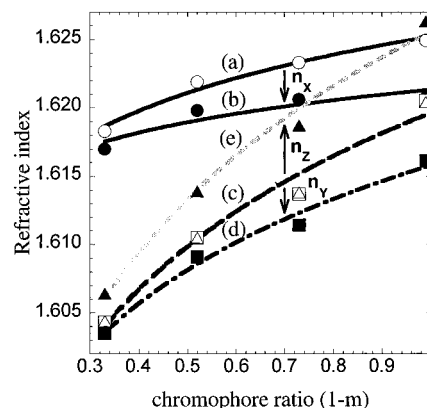


**Figure 12.** Refractive indices of drawn and poled polymer films as a function of chromophore ratio: (a)  $n_X$  (before poling); (b)  $n_X$  (after poling); (c)  $n_Y$  and  $n_Z$  (before poling); (d)  $n_Y$  (after poling); (e)  $n_Z$  (after poling). All samples were drawn by 2.3 times, and poled films were applied by 150 V/ $\mu$ m at  $T_g - 17^\circ\text{C}$ .

and poling using the novel phenoxy polymer containing 4-nitrophenylcarbamate as the side chain.

## Conclusions

The novel functionalized side-chain polymers wherein 4-nitrophenylcarbamate is introduced into phenoxy resin were synthesized. Using these polymers, in-plane and out-of-plane birefringence could be controlled by drawing and poling. The factors for the control of in-plane and out-of-plane birefringence depend on chromophore ratio, draw ratio, and poling voltage. The chromophore ratio can control both types of birefringence, the draw ratio can control in-plane birefringence, and the poling voltage can control the out-of-plane birefringence only. Therefore, in-plane and out-of-plane birefringence can be controlled independently by these three factors. In conclusion, out-of-plane birefringence was increased with the applied electric field of contact poling and was independent of the drawing ratio in the case of uniaxial drawing. And almost drawn and poled polymer films showed the relation of refractive indices such as  $n_X > n_Z > n_Y$ .

**Acknowledgment.** We would like to thank Dr. Mochida (ORC Manufacturing Co. Ltd.) and New OJI Paper Co. Ltd. for measuring the refractive index. Also, we would like to thank Tohto Kasei Co. Ltd. for supplying the phenoxy resin.

## References and Notes

- (1) Samuels, R. J. *Structured Polymer Properties*; John Wiley & Sons: New York, 1974.
- (2) Krevelen, D. W. *Properties of polymers, their estimation and correlation with chemical structure*, 2nd ed.; Elsevier Scientific Publishing Co.: Amsterdam, 1976.
- (3) Tanaka, T.; Inoue, T. *J. Non-Cryst. Solids* **1991**, 131–133, 781.
- (4) Khohei, A. (Fuji Photo Film Co.) Jpn. Kokai Tokkyo Koho (Patent) JP-A-160204, 1990.
- (5) Hiroyuki, Y. (Nitto Denko Co.) European Patent Application EP-A-2-482620, 1992.
- (6) Umemoto, S.; Fujimura, Y.; Yamamoto, H. (Nitto Denko Co.) Jpn. Kokai Tokkyo Koho (Patent) JP-A-285303, 1990.
- (7) Fujimura, Y.; Nagatsuka, T.; Yoshimi, H.; Umemoto, S.; Shimomura, T. *SID' 92 Digest* **1992**, 397.
- (8) Hanna, D. C.; Yuratich, M. A.; Cotter, D. *Nonlinear Optics of Free Atoms and Molecules*; Springer-Verlag: Berlin, 1981.
- (9) Singer, K. D.; Sohn, J. E.; Lalama, S. J. *Appl. Phys. Lett.* **1986**, 49, 248.



- (10) Perrin, D. D.; Armarego, W. L. F.; Perrin, Dawn, R. *Purification of laboratory chemicals*, 2nd Ed.; Pergamon Press: New York, 1980.
- (11) Ulrich, R.; Torge, T. *Appl. Opt.* **1973**, *12*, 2910.
- (12) Tien, P. K. *Appl. Opt.* **1973**, *10*, 2395.
- (13) Polky, J. N.; Mitchell, G. L. *J. Opt. Soc. Am.* **1974**, *64*, 274.
- (14) Hayashi, A.; Goto, Y.; Nakayama, M.; Kaluzynski, K.; Sato, H.; Watanabe, T.; Miyata, S. *Chem. Mater.* **1991**, *3*, 6.
- (15) Hayashi, A.; Goto, Y.; Nakayama, M.; Kaluzynski, K.; Sato, H.; Kato, K.; Kondo, K.; Watanabe, T.; Miyata, S. *Chem. Mater.* **1992**, *4*, 455.
- (16) Bloembergen, N.; Pershan, P. S. *Phys. Rev.* **1962**, *128*, 606.
- (17) Jerphagnon, J.; Kurtz, S. K. *Phys. Rev.* **1970**, *B1*, 1739.
- (18) Oudar, J. L.; Zyss, J. *Phys. Rev. A* **1982**, *26*, 2016.
- (19) Stewatt, J. J. P. *J. Comput. Chem.* **1989**, *10*, 209.
- (20) Pople, J. A.; Beveridge, D. L. *Approximate Molecular Orbital Theory*; MacGraw-Hill: New York, 1970.
- (21) Reinking, N. H.; Barnabeo, A. E.; Hale, W. F.; Mason, J. H. *J. Appl. Polym. Sci.* **1963**, *7*, 2153.
- (22) Sugihara, O.; Nakayama, H.; Okamoto, N.; Sakakibara, T.; Taketani, Y. *Jpn. J. Appl. Phys.* **1994**, *33*, L321.
- (23) Stähelin, M.; Walsh, C. A.; Burland, D. M.; Miller, R. D.; Twieg, R. J.; Volksen, W. *J. Appl. Phys.* **1993**, *73*, 8471.
- (24) Mortazavi, M. A.; Knoesen, A.; Kowel, S. T.; Higgins, B. G.; Dienes, A. *J. Opt. Soc. Am.* **1989**, *B6*, 733.
- (25) Nye, J. F. *Physical Properties of Crystals*, Oxford University Press: London, 1967; pp 116–122.
- (26) Parasad, Paras N.; Williams, D. J. *Introduction to Nonlinear Optical Effects in Molecules & Polymers*; Wiley-Interscience: New York, 1989; pp 67–73.
- (27) Tao, X. T.; Watanabe, T.; Zou, D. C.; Miyata, S. *J. Opt. Soc. Am.* **1995**, *B12*, 1581.
- (28) Kotler, Z.; Hierle, R.; Josse, D.; Zyss, J. *J. Opt. Soc. Am.* **1992**, *B9*, 534.
- (29) Choy, M.; Beyer, R. L. *Phys. Rev.* **1976**, *B14*, 1693.
- (30) Williams, D. In *Nonlinear Optical Properties of Organic Molecules and Crystals*, Chemla, D. S., Zyss, J., Eds.; Academic: Orlando, FL, 1987; p 405.
- (31) Kuzyk, M. G.; Singer, K. D.; Zahn, H. E.; King, L. A. *J. Opt. Soc. Am.* **1989**, *B6*, 742.
- (32) Tasaka, S.; Ohishi, K.; Nalwa, H. S.; Watanabe, T.; Miyata, S. *Polym. J.* **1994**, *26*, 505.
- (33) Desper, C. R.; Stein, R. S. *J. Appl. Phys.* **1966**, *37*, 3990.
- (34) Takahara, H.; Nomura, S.; Kawai, H.; Yamaguchi, Y.; Okazaki, K.; Fukushima, A. *J. Polym. Sci.*, **1968**, *A-2*, *6*, 197.
- (35) Taylor, G. R.; Darin, S. R. *J. Appl. Phys.* **1955**, *26*, 1075.

MA960285T